Journal of Advanced Engineering Trends
ISSN : 2682 - 2091

Vol. 44, No. 1, January 2025

PV-Based off Grid Valve Drive System for Leakage Protection in Water Networks

Aya A. M. Teleb[1], Mohamed Reda Mahmoud[1,2*], Gamal M. Dousoky[1, 3]

[1]*Electrical Engineering Dep., Faculty of Engineering, Minia University, Minia, Egypt*
[2] *Electromechanical Systems, and Metal Engineering Dep., Ghent University, Ghent, Belgium*
[3] *Mechatronics Engineering Dep., Nahda University, Beni-Suef, Egypt*
** Corresponding author(s) E-mail: mohamed.hassan@mu.edu.eg*

ARTICLE INFO

Article history:
Received: 2 April 2024
Accepted: 8 July 2024
Online: 1 January 2025

Keywords:
Photovoltaic
PI controller
Standalone
Battery

ABSTRACT

This paper proposes a PV-based off-grid valve drive system for leakage protection in water networks. The system integrates photovoltaic panels, energy storage units, and motorized valve control mechanisms to ensure reliable and efficient operation. The PV panels harvest solar energy, which is stored for use during low-light conditions or at night. A motorized valve control mechanism driven by the stored energy actively manages valve opening and closing based on leakage detection sensor measurements. Moreover, maximum power point tracking (MPPT) for the PV panels is set to maximize the system efficiency. Then, power management is designed to control the power flow between the different system units and keep the valve actuator voltage constant under different operation conditions. Simulation results demonstrate the system's effectiveness in detecting and isolating leakage, reducing water loss, and minimizing system downtime. Furthermore, the system's off-grid nature enhances resilience against power disruptions, making it a sustainable solution for leakage protection in water networks.

Nomenclature

A	Battery voltage exponential zone amplitude	P_{PV}	PV generated power
A_{PV}	Diode ideality factor	Q	Capacity of the battery
B	Battery voltage exponential zone time constant inverse	q	Electron charge
E_0	Battery constant voltage	$\mathrm{Q_{In}}$	Water flow rate at the inlet of the water network
I	PV module current	$\mathrm{Q_{Out}}$	Water flow rate at the outlet of the water network
I_{Bat}	Battery current	R	instantaneous resistance
I_{ph}	PV generated current by photo-effect	R_{inc}	Incremental resistance
I_s	Saturation current of the PV diode	R_{int}	Battery internal resistance
K	Boltzman's constant	R_p	Parallel PV cell resistance
K_{Bat}	Polarization voltage of the battery	R_s	Series PV cell resistance
L	Bi-directional buck-boost inductance	SoC	Battery state of charge
L_{Boost}	MPPT boost inductance	SoC_{int}	Battery initial state of charge
N_p	Number of parallel connected PV cells	T	PV module ambient temperature
N_s	Number of series-connected PV cells	V	PV module voltage
P_{Bat}	Battery power	V_{Bat}	Battery terminal voltage
P_{Load}	Load (motorized valve) power		

1. Introduction

Water is an important natural resource. It is an extension of the existence of all living beings and cannot be discarded. The importance of water is not limited to the basic drink of living beings but is due to its chemical properties, which are not found in any other drink. Therefore, every effort must be made to save it from any leakage[1, 2].

The development of a city is substantially influenced by the availability of water, and urbanization has an enormous effect on those resources, causing a decrease in quantity, guaranteeing the

end users of high-quality water, and a decline in water quality [3]. To meet the rising demand for water, particularly in emerging nations, new water facilities and supply infrastructure must be built. So, controlling water leaks in distribution systems is an important task for protecting water resources, particularly in light of water shortage and climate change [1]. Related advantages include a decrease in energy utilization and greenhouse gas emissions. From this perspective, preventing water leaks can boost the economy and advance social objectives [3].

In the following literature, several methods used for fluid leakage detection in pipelines are presented. Traditionally, measuring the difference in the volume of water entering the pipeline and the volume of water at the receiving end estimates the leakage [4]. The acoustic method makes use of a sensor that is based on an acoustic-detecting component and detects noise inside the pipe. The sensor wirelessly transmits the signals it has picked up to a gateway that is located on the ground. These signals are then transmitted to a backend server by the gateway. The primary site where data is transformed into information and presented to the user is the backend server [5, 6]. This technique avoids service interruption, not only detecting leaks but also pinpointing their positions and detecting leaks of varying sizes and locations. But ground-surface listening devices must be almost directly over a leak location to be effective, accuracy depends on the field technician, and results vary depending on the material and depth of the pipeline, type of soil, etc.

The infrared thermography method employs a thermal (IR) camera to image and measure an object's emitted infrared radiation. The basic idea for this method is that water leaking from a pipe under the ground affects the thermal properties of the surrounding soil [7]. Infrared cameras can detect this change in thermal properties as well as thermal contrasts on the pavement surface caused by water leaks. Thermography allows for the monitoring of relatively wide areas in less time and at a lower cost. It is also independent of pipe size and type and can be utilized at any time of day or night [7]. On the other hand, is affected by weather, soil, pavement surface characteristics, groundwater level, and distance between sensor and source. The user's experience is particularly important. Analyzing the image also necessitates a certain level of experience [8].

In the Thermal (IR) imaging-based wireless sensor method, each segment of the pipe, which is housed inside a duct, will be connected with a sensor unit that consists of a thermal imaging camera and an RF transceiver. The local image processing will determine if there is a leak in that length of pipe after the thermal imaging camera periodically captures the image, such as once per day. The observed information is then transmitted to the main base station using the RF Trans receiver [7]. This technique of low-cost, low-power thermal imaging sensors, operating independently of pipe type, size, weather, or surface conditions, has the capacity to operate in low lighting or dark conditions, and identify leaks very early [7].

The installation of a fiber optic cable to measure the temperature along the whole length of the pipeline is part of the fiber optic sensing leakage detection method. Usually, leaks from pipes cause localized temperature anomalies near the pipeline [9]. The temperature profile along the fiber is determined by quickly scanning it throughout its full length, and the leaking point can then be found [9]. This technique offers accurate leakage detection and location[10], higher sensitivity and a wide range of safety applications, effectiveness in locating the leak, and reasonably quick response [2]. However, the price of installation is rather significant, can only be used to monitor linear pipelines [9], and is incapable of calculating the magnitude of the leak [11].

In [10] Sensors are used for the Magnetic Induction (MI) approach inside as well as outside of the pipelines. The temperature, humidity, and soil characteristics around underground pipelines are measured by sensors on the outside, while those inside measure pressure, fluid velocity, and acoustic vibrations caused by leaks. Magnetic induction transceivers are installed in pipeline sensors to allow them to connect with sensors buried throughout the pipeline. A wire coil is used to achieve magnetic induction communication. A sinusoidal current modulates the signal in the transmitter coil, creating a magnetic field in the transmitter's near field that changes over time. The communication is carried out by a second sinusoidal current being induced by the time-varying magnetic field in the receiver. Although MI systems provide accurate real-time leakage localization and detection results in challenging underground conditions, their performance necessitates a large number of sensors, which increases the cost of deployment.

The ground penetration radar (GPR) method is a technique that uses high-frequency electromagnetic wave propagation to detect changes in the electrical and magnetic properties of the soil surrounding the pipeline [9, 12]. GPR generates electromagnetic radiation, which travels through the earth before circling back to the surface. The sub-surface's dielectric constant affects the speed at which the radar waves move. Variations in the subsurface material and/or circumstances cause variations in the dielectric constant, which results in reflections. Interpreting this reflected energy can therefore reveal details about the underlying structural variation and medium condition[12]. This method is quick, independent of the kind of pipe, and it may be used with both metallic and plastic pipes [12]. However, this comes at a high cost, and the usefulness of deeply underground pipelines is constrained since either soil moisture or soil inhomogeneity may not be able to produce enough signal power levels above the noise floor [8].

The tracer gas technique uses external injecting of a non-hazardous gas into the water network under pressure to detect a pipeline leakage. The water that escapes at the leak point also contains the gas and is detected by a spectrometer and electronic nose [7]. Typically, another pipeline with built-in sensors is put beside the pipeline that needs to be monitored so that, in the event of a leak, the sensors can quickly warn the engineers. [8]. This method is independent of the type of pipes, the soil, and the weather [5], and can detect extremely small leaks[9]. However, the vast amount of gas required prevents employing this technology in large low-pressure applications [9], and it may harm environmental contamination in the presence of a leak [8, 10].

In [13], Two flow sensors are utilized in this system, one at the beginning of the pipeline and one after the pipeline. The Arduino controller is used to control the entire gadget as well as collect data

from linked devices. If there is a leak in the pipeline, the water flow rate of flow sensor 2 differs from flow sensor 1, and the GSM module can transmit an alert message to the main server room. Using this method, water breaks in underground pipelines can be identified instantly, and the user can monitor the pressure level of water inside the pipeline.

In this article, the flow rate measurement method is chosen, because it is economical and low cost due to the components are affordable, easy to assemble due to the constitution of the modules, and the overall system can operate in different operating systems[14]. This method has the ability to allow early detection of water leakage due to constant analysis and therefore can detect any water leakage accurately from the analysis[15]. The main aim of the system is reducing the leakage of water, so more benefits for both consumers as well as Water Corporation. Using the system water wastage can be reduced and save the water for the next generations[13]. This system not only conserves the water but also saves energy by having the pump automatically off.

Using the potential of off-grid photovoltaic systems is a viable option to provide electrical energy to regions that are remote from the national power grid [16]. Using solar radiation to produce electricity is a major approach to achieving sustainable energy resources in many parts of the world. The process of converting the energy stored in solar radiation to electrical energy is known as photovoltaic technology, and it is an appropriate alternative to conventional methods of generating power [16].

In off-grid systems, excess energy produced by photovoltaic panels can be stored in batteries to meet demand in a supply deficit. It is evident that using this type is sensible when the consumers are far from the grid or their access to the grid is difficult or unavailable. The main advantage of this type is that photovoltaic systems can deliver demand loads 24 hours a day. To fulfill the rapidly expanding demand for energy while reducing CO_2 emissions, more renewable energy sources and other low-carbon energy sources will become major contributors to the future power system [17]. Solar energy, which is environmentally friendly, clean, and requires no maintenance, is an alternative renewable energy source, particularly for nations with high yearly solar irradiation rates, such as Egypt [18].

One of the methods used to improve the PV system's efficiency is applying maximum power point tracking (MPPT). Perturb and Observe (P&O) MPPT technique is one of the commonly used methods. In [19] [20], improving the MPPT algorithm based on the P&O framework was implemented. On the other hand, a simplified and robust MPP algorithm based on incremental conductance (INC) was presented in [21] in order to minimize the complexity. Ref. [22] presented a hybrid MPPT method based on INC using an integral backstepping controller. However, this method suffers from nonlinearity and high computational time. A simplified buck power control algorithm was used to emulate the PV panels in efficient and rapid computational manners as presented in [23, 24].

The current article's contribution can be summaries as follows:

- Reviewing the different water leakage detection methods.
- Designing a renewable energy system to supply the valve actuator.
- Applying MPPT to maximize the power generated by the PV module.
- Energy management for the PV battery system to control the charging/discharging of the battery under different operating conditions.

This article is arranged into sections that can be summarized as follows: Section (2) presents the water network system. Section (3) discusses the motorized valve actuator. Section (4) presents the standalone PV system (modeling, sizing, and control). Section (5) illustrates the test results of the system. Finally, Section (6) reports the conclusions of the research.

2. Water network system

In this article, a real water pipeline that is used as the main feeding water pipeline, for the village of Maqoussa which is located in Minya-Egypt, is studied under leakage conditions. The feeder is a 1.20 m water pipeline with a water pressure of about 2-4 bar. This water feeder frequently leaks three times a year and takes about three working days to fix it. The water leakage in this feeder causes a lot of damage to environmental resources and makes people life more difficult. Continuous and frequent water leakage in the same area causes damage to homes and buildings around the site of the leakage. [e.g. Figure 1, shows the damage caused to the infrastructure of the village to find out the leakage and repair it]. Figure 2, presents a line diagram for the described water feeder. The parameters of the water pipeline are given in Appendix A.

Figure 1: Actual case infrastructure damage.

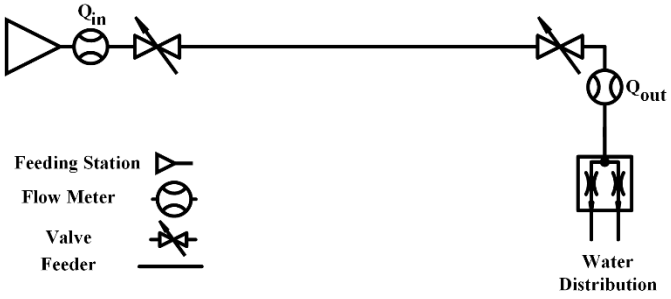

Figure 2: Block diagram of the water feeding system.

3. Valve Drive system

The used valve actuator in this research is a motorized valve. DC motor valve drive systems are widely used in different industries such as manufacturing, oil and gas, treatment of water, and HVAC (heating, ventilation, and air conditioning), among

others. They offer reliable and precise control over valve operations, allowing for efficient regulation of fluid flow and process control[25].

4. Off-grid photovoltaic energy systems

To study the performance of the proposed standalone PV system used to supply a motorized valve actuator. This involves understanding the performance of the system under different operating conditions, during both high and low irradiance conditions, and controlling the flow of energy between the PV panels, batteries, and load. In this article, the proposed standalone PV system mainly comprises PV and battery as presented in Figure 3. The batteries are used as energy storage to supply the motorized valve in case of a trip during sunset conditions. Both the PV and batteries are connected to the dc bus through MPPT boost converter, and bi-directional buck-boost converter, respectively. The modeling of the system units is introduced in the following subsections:

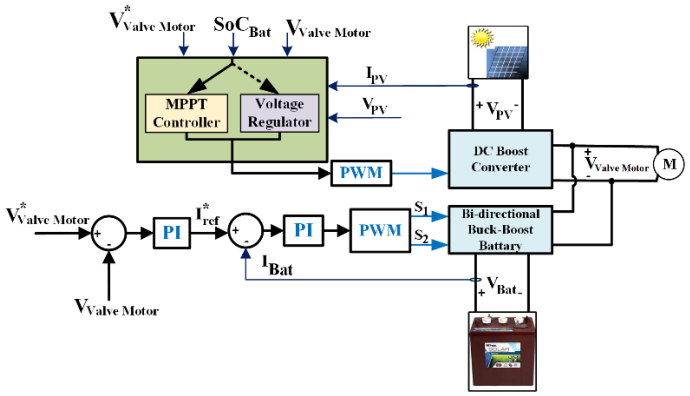

Figure 3: Block diagram of the standalone system

4.1. Photovoltaic module

The single-diode model is a widely used electrical model for PV cells and modules as shown in Figure 4. It represents the current-voltage (I-V) characteristics of a PV device considering various parameters such as the diode ideality factor, series and shunt resistances, and the effects of temperature and solar irradiance[26, 27]. The i-v characteristics of the PV module can be described by:

$$I = N_P\left[I_{ph} - I_s\left\{\exp\left(\frac{q}{A_{PV}KT}\left(\frac{V}{N_s} + \frac{I}{N_p}R_s\right)\right) - 1\right\} - \frac{\frac{V}{N_s}+\frac{I}{N_p}R_s}{R_p}\right] \quad (1)$$

where I and V are the PV module current and voltage, respectively. I_{ph} is the current generated by photo-effect; I_s is the saturation current of the diode; q is the electron charge ($1.6 \times 10^{-19}\ C$); A_{PV} is the diode ideality factor; T is the module ambient temperature in Kelvin; K is Boltzman's constant ($1.38 \times 10^{-23}\ J/C$); R_s and R_p are the series and parallel resistance; and N_s and N_p are the number of series and parallel connected cells.

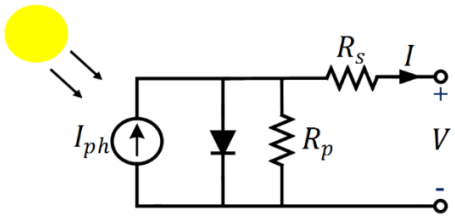

Figure 4: The PV module equivalent circuit

4.2. Battery storage

The Thevenin model represents a battery as an ideal voltage source in series with an internal resistance. It simplifies the battery behavior by considering it as a constant voltage source with a predictable voltage drop due to internal resistance as illustrated in Figure 5. The terminal voltage of the battery can be expressed as [28]:

$$V_{Bat} = E_0 - K\frac{Q}{Q - \int I_{Bat}dt} + Ae^{-B\int I_{Bat}dt} - R_{int} \times I_{Bat} \quad (2)$$

where E_0 is the battery constant voltage, K is the polarization voltage of the battery (V), Q is the capacity of the battery (Ah), A is the exponential zone amplitude (V), and B is the exponential zone time constant inverse (Ah^{-1}). The battery state of charge (SoC) is given by[29]:

$$SoC = SoC_{int} - \frac{1}{Q}\int I_{Bat}dt \quad (3)$$

where SoC_{int} is the battery initial state of charge.

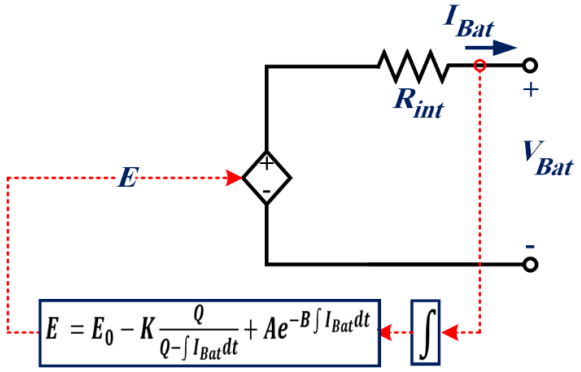

Figure 5: The Battery equivalent circuit

4.3. Power converters

In order to connect PV array, and battery with the DC load bus DC-DC converter are used. This promise a full control for both the PV and battery storage. The DC-DC converter that connects PV array with the load bus is boost converter. The bi-directional buck-boost converter is a good solution to connect the battery.

Figure 6 presented the power stage of the boost converter which is used to achieve maximum power point tracking (MPPT). It is consisting of a single pole double throw switch (SPDT), connected to a low pass filter which consists of smoothing inductance (L_{Boost}), and smoothing capacitor (C), which is connected between the PV array and the dc bus [27].

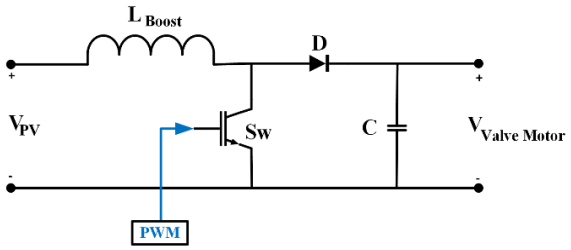

Figure 6: The power stage boost converter

The battery storage is connected to the dc load bus through the bi-directional buck-boost. This allows voltage control of the dc bus load as well as control of the battery instantaneously. Figure 7 illustrated the power stage of the converter which consists of two switches Q_1 and Q_2, smoothing inductance L and output smoothing capacitance C. It has two mode of operation: Buck mode during charging the battery; and boost mode during discharging the battery. During buck converter mode, the current flows from the dc load bus to the battery and the switch Q_2 is always OFF. By controlling the duty cycle D_1 of the switch Q_1, the converter decreases the dc load bus voltage in order to charge the battery. In boost mode, the current flows from the battery to the dc load bus and the switch Q_1 is always OFF. By controlling the duty ratio D_2 of the switch Q_2, the converter can increase the battery voltage to the dc load bus voltage. The design parameters that size the both the boost and bi-directional buck-boost converters are given in appendix A.

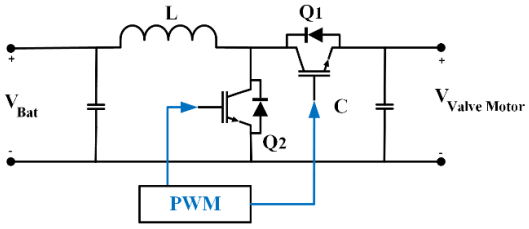

Figure 7: The power stage of bi-directional buck-boost

4.4. PV battery system sizing

It is important to accurately size both the PV array and the battery storage to ensure that the system is able to provide the continuous power required by the motorized valve load in normal conditions without surge current under different operating conditions. In order to supply this load, the PV array, storage battery, and dc-dc converters are designed, and accordingly sized as illustrated in Tables 1, 2, and 3.

Table 1. The PV array sizing specifications.

PV array power	PV module power	PV module MPP voltage	PV module MPP current	No. of series modules	No. of parallel branches
1040 W	130 W	17.38V	7.43 A	2	4

Table 2. The battery storage sizing specifications.

Battery voltage	Battery capacity	Required battery capacity	No. of series batteries	No. of parallel branches
12 V	150 Ah	300 Ah	2	1

Table 2. The DC-DC converters parameters.

Component \ Converter	Bi-directional battery converter	MPPT boost converter
Inductance	0.2 mH	0.25 mH
Switching frequency	16 kHz	16 kHz
Low voltage	24 V	PV output voltage
High voltage	48 V	48 V
Low voltage side capacitor	16 µF	100 µF
DC load bus capacitor	100 µF	

4.5. Boost converter control

The boost converter, connects PV array with the load bus, is controlled to achieve MPPT except in case of the battery is out of service due to low SoC or full charge the boost converter operates as voltage regulator. In the following points, the operation of both MPPT and voltage regulator will be introduced:

A. MPPT Algorithm

In this study, the incremental resistance (INR) MPPT method is applied. This technique is based on the concept that the MPP occurs when the incremental resistance of the solar panel is equal to the negative of the instantaneous resistance [30, 31]. The steps of INR-MPPT is as following:

i. Initial step: Measure the initial PV voltage and current.
ii. Iterative steps:
- Measure the new PV voltage V_{new} and current I_{new}.
- Calculate the change in voltage ($\Delta V = V_{new} - V$) and current($\Delta I = I_{new} - I$).
- Calculate the incremental resistance $\left(R_{inc} = \frac{\Delta V}{\Delta I}\right)$ and instantaneous resistance $\left(R = \frac{V_{new}}{I_{new}}\right)$.

iii. Decision making:
- Compare the incremental resistance and the negative of instantaneous resistance to make decision as follows:

$$\begin{cases} R_{inc} = -R & \rightarrow \quad \text{MPP is reached} \\ R_{inc} > -R & \rightarrow \quad \text{decrease the PV voltage} \\ R_{inc} < -R & \rightarrow \quad \text{increase the PV voltage} \end{cases}$$

- Adjust the boost converter duty cycle accordingly to match these cases.

iv. Repeat: Repeat the process continuously tracking the MPP.

B. Voltage Regulation

The output of the PV array is controlled to obtain constant load voltage in case of battery deficit. A PI controller is used to regulate the voltage to the reference value. The voltage regulator using PI controller is presented in Figure 8 where the PI controller gains are given in appendix A.

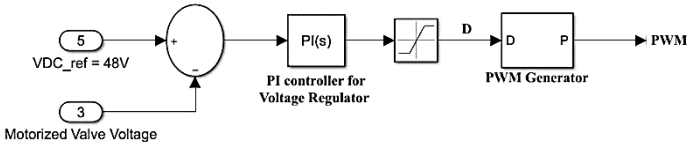

Figure 8: Boost converter voltage regulating PI controller.

4.6. Control strategy

The flow chart presented in Figure 9 illustrates the operation of the controller used to control the load bus, the MPPT of the PV, and the battery. The battery charges when the PV power is large than the load requirements ($P_{PV} > P_{Load}$). On the other hand, the batteries tend to discharge in cases of insufficient available PV power to fulfill the load demand ($P_{PV} < P_{Load}$).

The following considerations are taken into account during the power control design:

- The main task of the battery and the associated bi-directional converter is to regulate the load dc bus voltage and supply the load demand in case of PV power deficit.
- The system is designed to increase the surplus PV power by charging both battery until they reach their maximum affordable SoC.
- If the battery is out of service due to low SoC, the PV boost converter operates as voltage regulator to compensate the absence of battery.
- If the available PV power is higher than the load demand, the PV converter operates as a MPPT, and accordingly, the battery is allowed to charge until the maximum permissible SoC is reached.

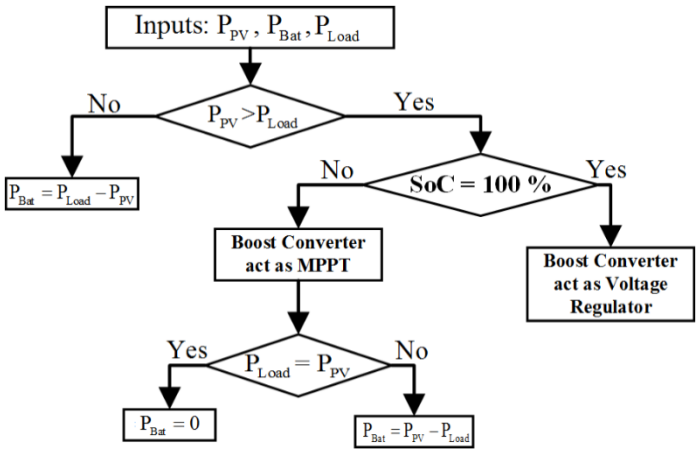

Figure 9: The Controller flow chart

5. Simulation and Results

To investigate the overall performance of the proposed system, the water network in addition to the PV hybrid system that is used to supply the valve drive system is simulated using the MATLAB-Simulink software packages. The parameters of the PV module, battery storage unit, test pipe, motorized valve actuator and the controllers are presented in appendix A.

The measurement of water flow rate at both the inlet and outlet of the system are shown in Figure 10, are the same before the leakage is detected at the 1 s. The leakage is detected at 1 s since the inlet and outlet flow rates are not equal. This figure also ensures that the flow rate becomes zero after clearing the leakage by closing the valve. Figure 11, illustrates the leakage detection signal which is a trip signal to the motorized valve actuator in order to operated and close both valves to save water.

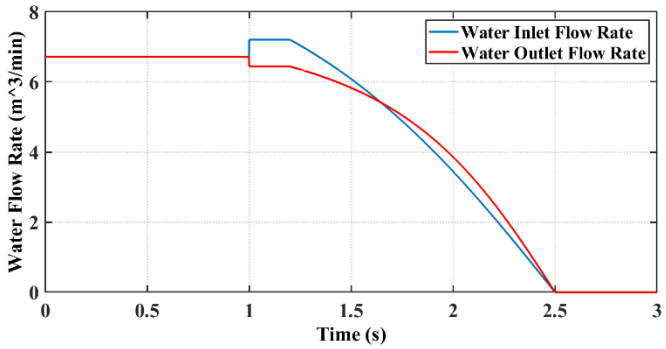

Figure 10: The water flow rate waveform.

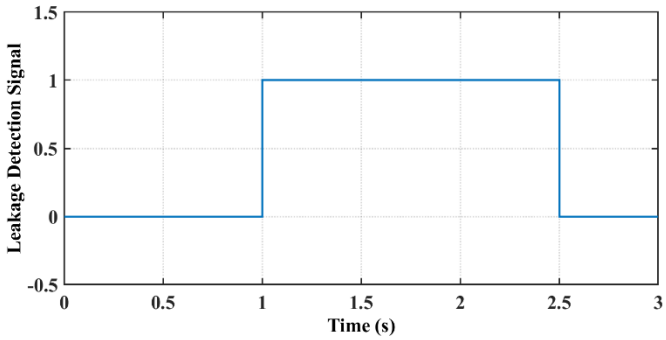

Figure 11: The leakage detection signal

The solar irradiance, presented in Figure 12, is assumed to be varied from 1000 W/m^2 (i.e., sunny day) to 700 W/m^2 (i.e., cloudy day). The motorized valve actuator voltage and current are presented in Figures 13-14, respectively. The voltage across the load bus (motorized valve actuator terminal voltage) presented in Figure 12. This reports that the voltage across the valve actuator is kept constant under different operating conditions such as the change of both irradiance and load current. Figure 14 presents the motorized valve actuator current which validate that the valve draws current only during clearing the leakage.

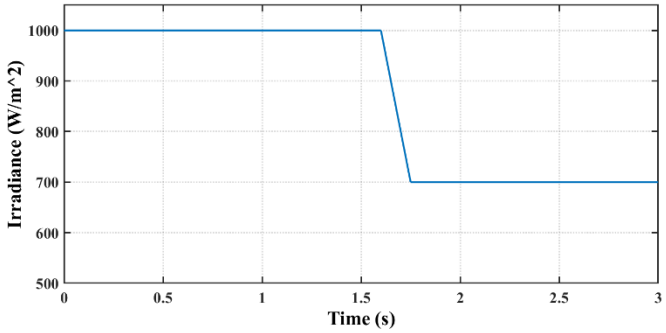

Figure 12: The solar radiation

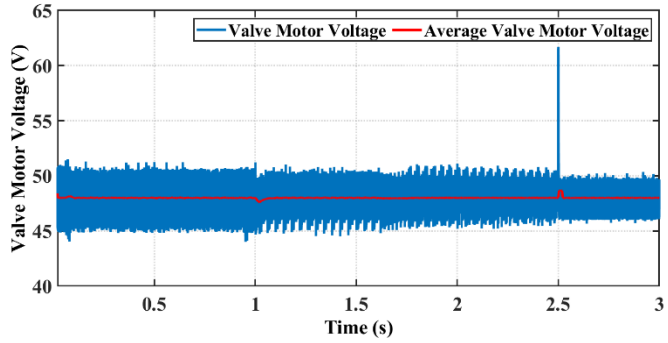

Figure 13: The load bus voltage waveform.

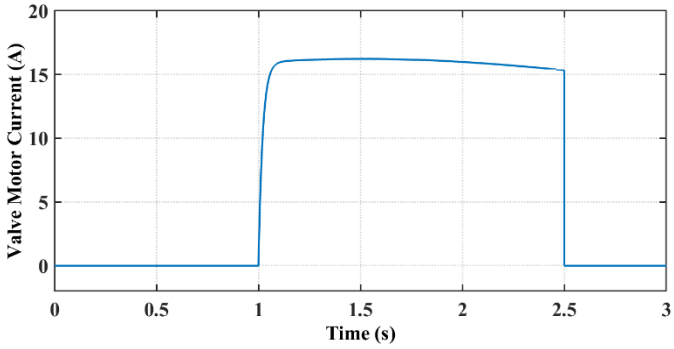

Figure 14: The motorized valve current waveform.

Figure 15, Figure 16 and Figure 17 illustrate the performance of the PV array in terms PV voltage, PV current, and the duty ratio of the MPPT boost converter. The MPP tracking response, is clearly presented in both high- and low-solar radiation levels. Both the voltage and current of the PV system have better response under both the change of radiation and load. These figures ensure the MPP operation of the boost converter.

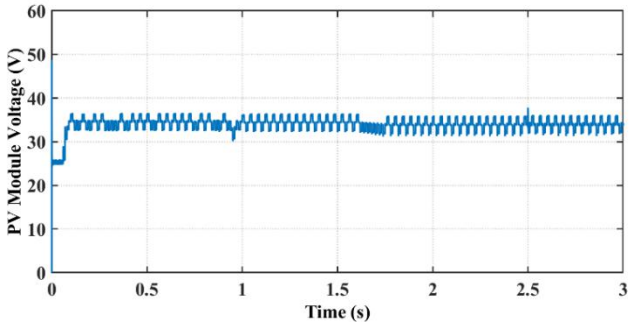

Figure 15: PV array voltage waveform.

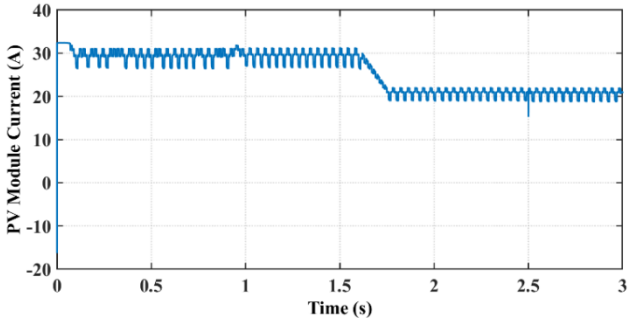

Figure 16: PV array current waveform.

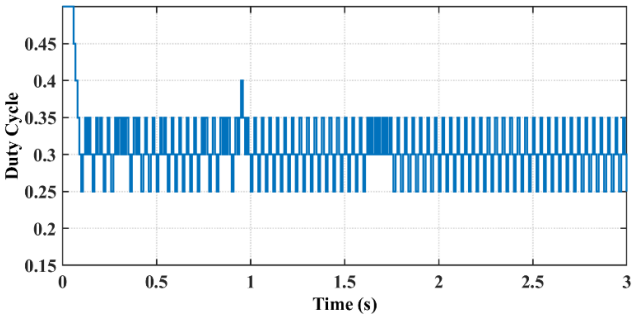

Figure 17: The MPPT boost converter duty ratio.

Figure 18, Figure 19 and Figure 20 illustrate the performance of the battery in terms battery terminal voltage, battery current, and the battery state of charge. The battery voltage fluctuation is acceptable according to charging/discharging conditions. The battery currents that reports the charging and discharging of the battery.

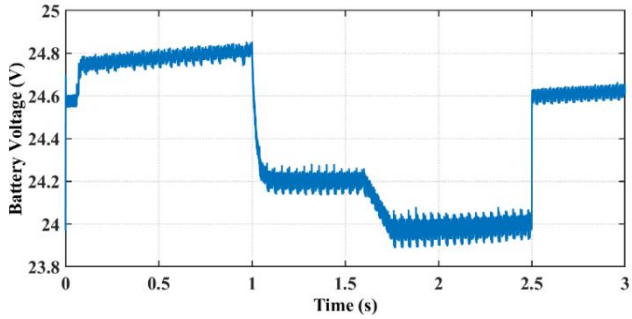

Figure 18: The battery voltage waveform.

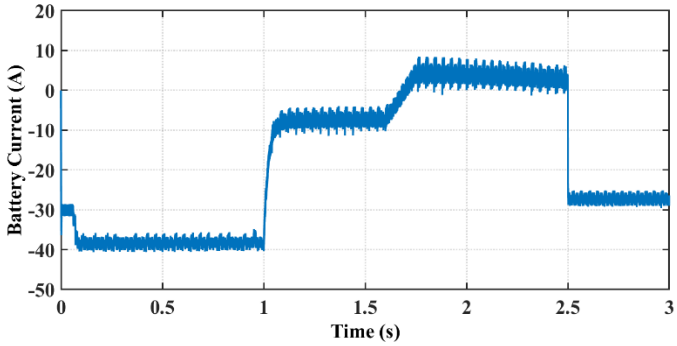

Figure 19: The Battery current waveform.

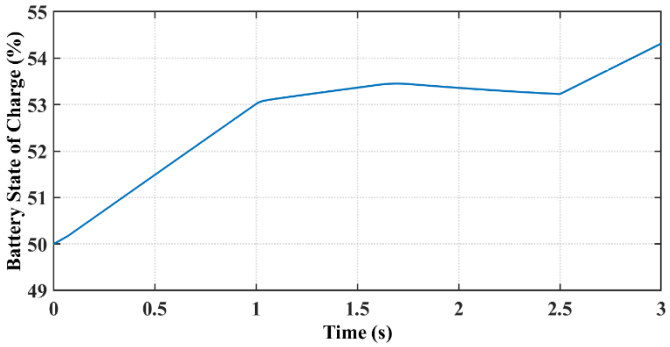

Figure 20: The battery state of charge.

Figure 21 illustrates the power diagram of the standalone system. This figure ensures the power balance of the system. In the first 1 s, the generated power from PV equals the power that charge the battery. When the leakage is detected at 1s, the valve motor start and the battery power become the difference between the PV power and the motor power. When the radiation decreased, the battery provides the PV power deficit.

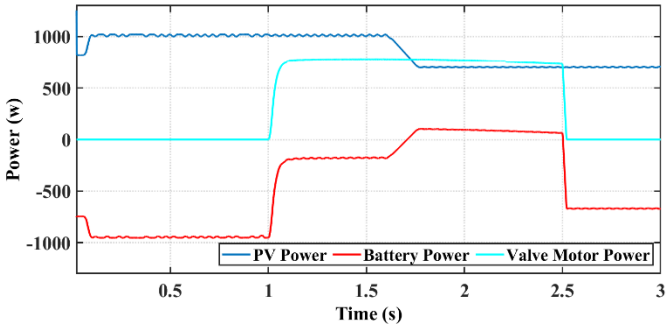

Figure 21: Power diagram of the system.

6. Conclusions

This paper proposed using standalone PV system to supply the water valve actuators. First, a literature about the different methods used to discover the water leakage was introduced. Then, the difference in water flow rate method was implemented to detect the water leakage. Finally, a standalone PV system was designed to supply the water network actuators. The proposed method reduced the leakage amount of water. The proposed supply is reliable. The obtained results prove that the right operation of the MPPT under both high and low solar radiation. Furthermore, both the charging and discharging of the energy storage battery are validated under different operation conditions.

Conflict of Interest

The authors declare no conflict of interest.

Appendix A

The parameters of the test pipe, motorized valve actuator, PV module, battery storage unit, and the controllers are presented in Table A1.

Table A1: The system Parameters

Parameter	Value
Test Pipe	
Pipe length	2.5 km
Pipe diameter	1.2 m
Water pressure	2-4 bar
Pipe cross-sectional type	Circular
Geometric shape factor	64
Internal surface roughness height	0.5 mm
Motorized Valve Actuator	
Rated Power	750 W
Motor Rated Voltage	48 Vdc
Armature resistance	3 Ω
Armature inductance	0.061 H
Filed resistance	120 Ω
Field inductance	100 H
PV Module Parameters	
Peak Power P_{MAX}	130 W
Maximum Power Voltage	17.38V
Maximum Power Current	7.43 A
Open Circuit Voltage	22.07V
Short Circuit Current	7.86A
R_s	0.299 Ω
R_p	362.27 Ω
Nominal Operating Cell Temperature (NOCT)	44 °C
Temperature Coefficient of V_{OC}	- 0.296 %/°C
Temperature Coefficient of I_{SC}	0.123%/°C
Battery Parameters	
Battery constant voltage (E_0)	12.6463 V
Battery polarization constant (K)	0.33 V
Battery capacity (Q)	150 Ah
Battery exponential zone amplitude (A)	0.66 V
Battery exponential zone time constant inverse (B)	2884.6 $(Ah)^{-1}$
Internal resistance of the battery (R_{int})	0.1 Ω
Controllers Parameters	
Sampling period	10μs
Proportional gain (K_P) of the load bus voltage PI controller	1.22
Integral gain (K_I) of the load bus voltage PI controller	2288.25
Proportional gain (K_P) of the battery current PI controller	0.4
Integral gain (K_I) of the battery current PI controller	15.425
Proportional gain (K_P) of the voltage regulator PI controller	0.1
Integral gain (K_I) of the voltage regulator PI controller	1

References

[1] Q. Xu, R. Liu, Q. Chen, and R. Li, "Review on water leakage control in distribution networks and the associated environmental benefits," *Journal of Environmental Sciences*, vol. 26, no. 5, pp. 955-961, 2014/05/01/ 2014.

[2] S. Datta and S. Sarkar, "A review on different pipeline fault detection methods," *Journal of Loss Prevention in the Process Industries*, vol. 41, pp. 97-106, 2016/05/01/ 2016.

[3] R. Barnes, J. Skaalvik, M. Swilling, B. Robinson, S. Marvin, and M. Hodson, "City-Level Decoupling: Urban Resource

Flows and the Governance of Infrastructure Transitions," 2013.
[4] G. Dvajasvie, B. P. Farisha, S. N. Babu, K. P. Saheen, and N. C. Binoy, "Leak Detection in Water-Distribution Pipe System," in *2018 Second International Conference on Intelligent Computing and Control Systems (ICICCS)*, 2018, pp. 1-4.
[5] S. G. Kashid and S. A. Pardeshi, "A survey of water distribution system and new approach to intelligent water distribution system," in *2014 First International Conference on Networks & Soft Computing (ICNSC2014)*, 2014, pp. 339-344.
[6] A. Kadri, A. Abu-Dayya, R. Stefanelli, and D. Trinchero, "Characterization of an acoustic wireless sensor for water leakage detection in underground pipes," in *2013 1st International Conference on Communications, Signal Processing, and their Applications (ICCSPA)*, 2013, pp. 1-5.
[7] R. K. Parida, V. Thyagarajan, and S. Menon, "A thermal imaging based wireless sensor network for automatic water leakage detection in distribution pipes," in *2013 IEEE International Conference on Electronics, Computing and Communication Technologies*, 2013, pp. 1-6.
[8] T. K. Chan, C. S. Chin, and X. Zhong, "Review of Current Technologies and Proposed Intelligent Methodologies for Water Distributed Network Leakage Detection," *IEEE Access*, vol. 6, pp. 78846-78867, 2018.
[9] K. B. Adedeji, Y. Hamam, B. T. Abe, and A. M. Abu-Mahfouz, "Towards Achieving a Reliable Leakage Detection and Localization Algorithm for Application in Water Piping Networks: An Overview," *IEEE Access*, vol. 5, pp. 20272-20285, 2017.
[10] L. Boaz, S. Kaijage, and R. Sinde, "An overview of pipeline leak detection and location systems," in *Proceedings of the 2nd Pan African International Conference on Science, Computing and Telecommunications (PACT 2014)*, 2014, pp. 133-137.
[11] P.-S. Murvay and I. Silea, "A survey on gas leak detection and localization techniques," *Journal of Loss Prevention in the Process Industries*, vol. 25, no. 6, pp. 966-973, 2012/11/01/ 2012.
[12] S. Eyuboglu, H. Mahdi, H. Al-Shukri, and L. Rock, "Detection of water leaks using ground penetrating radar," in *Proceedings of the third international conference on applied geophysics, Orlando-FL*, 2003, pp. 8-12.
[13] W. A. Badawi, "Underground pipeline water leakage monitoring based on IOT," *International Journal of MC Square Scientific Research*, vol. 11, no. 3, pp. 01-08, 2019.
[14] R. Naveenkumar and P. Krishna, "Low cost data acquisition and control using arduino prototyping platform and LabVIEW," *International Journal of Science and Research (IJSR)*, vol. 2, no. 2, pp. 366-369, 2013.
[15] F. Ali and M. F. H. Saidi, "Water Leakage Detection based on Automatic Meter Reading," in *2021 15th International Conference on Ubiquitous Information Management and Communication (IMCOM)*, 2021, pp. 1-7.
[16] M. Davoudi, M. Moeini-Aghtaie, and H. R. Mosaddegh, "Introducing a novel method for improving the design of off-grid photovoltaic systems," in *2019 Smart Grid Conference (SGC)*, 2019, pp. 1-5.
[17] Y. Zong, L. Mihet-Popa, D. Kullmann, A. Thavlov, O. Gehrke, and H. W. Bindner, "Model Predictive Controller for Active Demand Side Management with PV self-consumption in an intelligent building," in *2012 3rd IEEE PES Innovative Smart Grid Technologies Europe (ISGT Europe)*, 2012, pp. 1-8.
[18] M. Dursun and S. Ozden, "Application of solar powered automatic water pumping in Turkey," *International Journal of Computer and Electrical Engineering*, vol. 4, no. 2, pp. 161-164, 2012.
[19] A. Harrison, C. Feudjio, C. Raoul Fotso Mbobda, and N. H. Alombah, "A new framework for improving MPPT algorithms through search space reduction," *Results in Engineering*, vol. 22, p. 101998, 2024/06/01/ 2024.
[20] J. d. D. Nguimfack-Ndongmo, A. Harrison, N. H. Alombah, R. Kuate-Fochie, D. Ajesam Asoh, and G. Kenné, "Adaptive terminal synergetic-backstepping technique based machine learning regression algorithm for MPPT control of PV systems under real climatic conditions," *ISA Transactions*, vol. 145, pp. 423-442, 2024/02/01/ 2024.
[21] T. Chen, A. Harrison, N. H. Alombah, M. Aurangzeb, S. Iqbal, and H. A. Mahmoud, "A simplified control algorithm for efficient and robust tracking of the maximum power point in PV systems," *Control Engineering Practice*, vol. 148, p. 105945, 2024/07/01/ 2024.
[22] A. Harrison, N. H. Alombah, and J. de Dieu Nguimfack Ndongmo, "A New Hybrid MPPT Based on Incremental Conductance-Integral Backstepping Controller Applied to a PV System under Fast-Changing Operating Conditions," *International Journal of Photoenergy*, vol. 2023, no. 1, p. 9931481, 2023/01/01 2023.
[23] N. Henry Alombah, A. Harrison, S. Kamel, H. Bertrand Fotsin, and M. Aurangzeb, "Development of an efficient and rapid computational solar photovoltaic emulator utilizing an explicit PV model," *Solar Energy*, vol. 271, p. 112426, 2024/03/15/ 2024.
[24] W. Zhu *et al.*, "A novel simplified buck power system control algorithm: Application to the emulation of photovoltaic solar panels," *Computers and Electrical Engineering*, vol. 116, p. 109161, 2024/05/01/ 2024.
[25] R. R. Henry, "Single-cylinder engine tests of a motor-driven, variable-valve actuator," SAE Technical Paper0148-7191, 2001.
[26] N. Pandiarajan and R. Muthu, "Mathematical modeling of photovoltaic module with Simulink," in *2011 1st International Conference on Electrical Energy Systems*, 2011, pp. 258-263.
[27] M. S. Hassan, S. Hassan, M. R. M. Hassan, A.-H. M. El-Sayed, M. Shoyama, and G. M. Dousoky, "Performance improvement of a standalone PV system using supercapacitors: modeling and energy management," *International Journal of Power Electronics and Drive Systems (IJPEDS)*, vol. 15, no. 1, pp. 222-238, 2024.

[28] M. R. M. Hassan, M. A. Mossa, and G. M. Dousoky, "Evaluation of Electric Dynamic Performance of an Electric Vehicle System Using Different Control Techniques," *Electronics*, vol. 10, no. 21, 2021.

[29] M. R. M. Hassan, M. Mossa, and G. M. Dousoky, "Dynamic Performance Analysis of An Electric Vehicle System Using Different Control Algorithms," (in en), *Journal of Advanced Engineering Trends*, vol. 43, no. 1, pp. 151-162, 2024.

[30] Q. Mei, M. Shan, L. Liu, and J. M. Guerrero, "A Novel Improved Variable Step-Size Incremental-Resistance MPPT Method for PV Systems," *IEEE Transactions on Industrial Electronics*, vol. 58, no. 6, pp. 2427-2434, 2011.

[31] L. Xu, R. Cheng, and J. Yang, "A New MPPT Technique for Fast and Efficient Tracking under Fast Varying Solar Irradiation and Load Resistance," *International Journal of Photoenergy*, vol. 2020, no. 1, p. 6535372, 2020/01/01 2020.